Figure S1. High NRF2 Activity Is Required for Efficient Spheroid Formation, Related to Figures 1 and 2.

(A) Percentage of RFP-positive cells cultured in 2D or 3D from three independent experiments. RFP-positive shControl or shNRF2 cells were co-cultured with parental cells. The cells were treated with 1 μg/ml doxycycline from two-day before the initiation of co-culture experiments to the end of the experiments. Two-way ANOVA was used to determine statistical significance ($^{**}p < 0.01$ and $^{***}p < 0.001$ compared to shControl). **(B)** Sequence of mutant *NFE2L2* (NRF2**) that is not targeted by shNRF2-#1 and mutant *NFE2L2* (NRF2*) that is not targeted by shNRF2-#2. **(C and D)** mRNA expression of NRF2 (C) and GCLC (D) in the indicated A549 and H1437 cells upon treatment with 1 μg/ml doxycycline for 72 hours. The cells were transduced with either an empty vector, NRF2*, or NRF2**. Data were normalized to the cells transduced with both shControl and an empty lentiviral vector and shown as mean ± SD from four independent experiments. **(E)** mRNA expression of NRF2 and NQO1 in the indicated cells upon treatment with 1 μg/ml doxycycline for 72 hours in 2D culture. Data were normalized to shControl. **(F)** Representative confocal images of the indicated day-20 H520 and day-16 SK-MES-1 spheroids stained with DAPI from two independent experiments. **(G)** Quantification of spheroid size from experiments described in (F) (n = 10–26). **(H)** Percentage of filled inner space in the indicated spheroids from experiments described in (F) (n = 9–16). **(I)** Representative confocal images of the indicated spheroids stained with DAPI from two independent experiments. The timeline of doxycycline treatment (1 μg/ml) is shown. **(J)** Percentage of filled inner space from experiments described in (I) (n = 18–21). **(K)** mRNA expression of NRF2 and GCLC in the indicated SK-MES-1 cells upon treatment with 1 μg/ml doxycycline for 72 hours in 2D culture. shControl or shNRF2-#1 cells were transduced with either an empty vector or mutant *NFE2L2* (NRF2**) that is not targeted by shNRF2-#1. Data were normalized to the cells transduced with both shControl and an empty vector. **(L)** Representative images of the indicated spheroids from two independent experiments. Scale bar represents 200 μm. **(M and N)** Representative confocal images of the indicated Day 12 (M) and Day 18 spheroids (N) stained with DAPI from two independent experiments. The timeline of doxycycline treatment (1 μg/ml) is also shown. **(O)** Quantification of spheroid size from experiments described in (M) (n = 102–169). **(P)** Percentage of filled inner space from experiments described in (N) (n = 52–100). **(Q)** Immunoblot analysis of NRF2 in the indicated H226 and H596 cells from two independent experiments. In (F–H) and (L), the spheroids were treated with 1 μg/ml doxycycline throughout the 3D culture. In (F), (I), (M), and (N), scale bar represents 100 μm. In (E), (G), (H), and (J), unpaired two-tailed t-test was used to determine statistical significance ($^{*}p < 0.05$ and $^{***}p < 0.001$ compared to shControl). In (C), (D), (K), (O), and (P), one-way ANOVA was used to determine statistical significance ($^{*}p < 0.05$, $^{**}p < 0.01$, and $^{***}p < 0.001$). In (E) and (K), data shown as mean ± SD from four independent experiments. All other data shown as mean ± SEM.
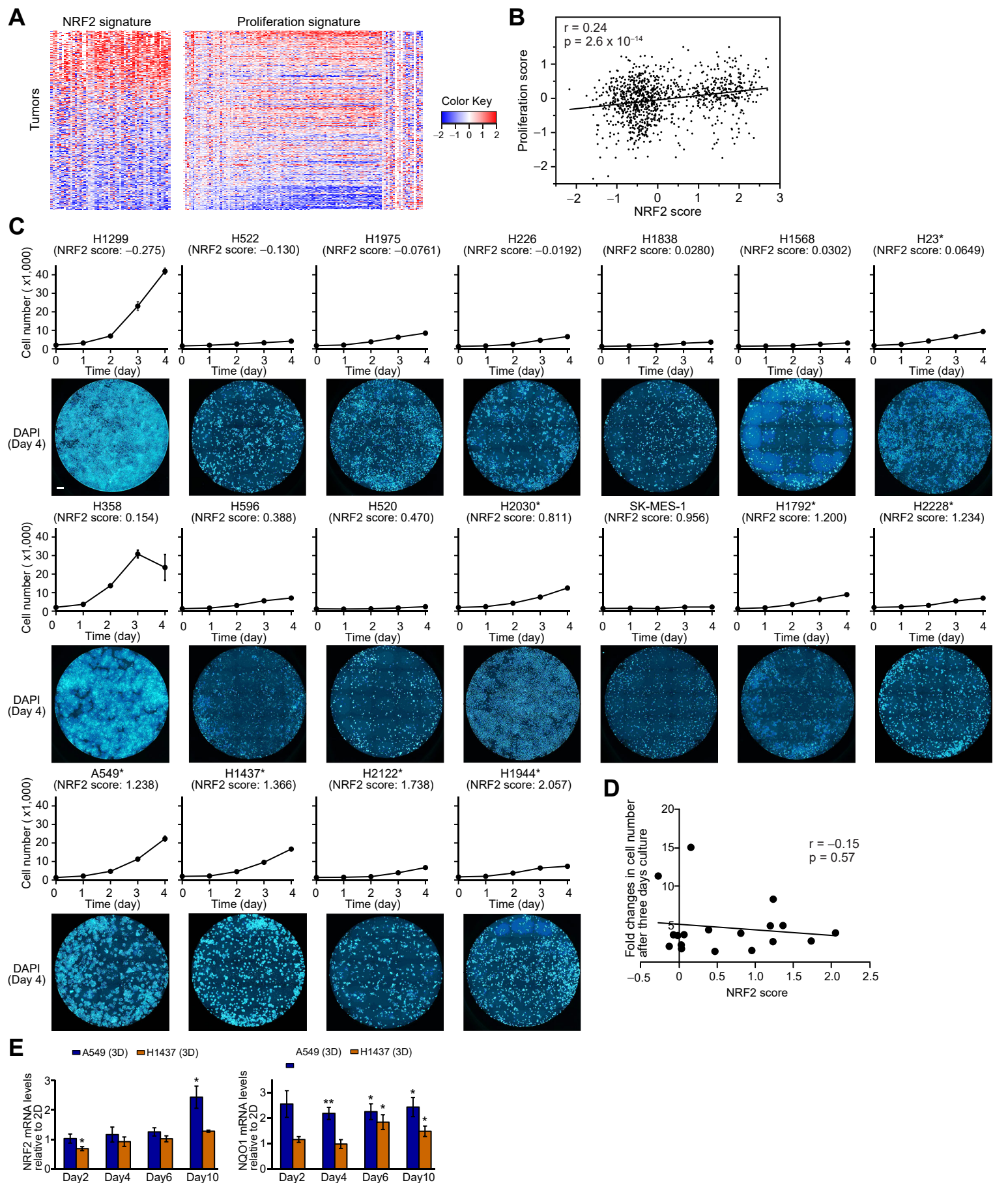
Figure S2. Correlation of NRF2 Signature with Proliferation Signature in Primary Patient Tumors and 2D monolayer cells, Related to Figures 2 and 3.

(A) Expression of NRF2 signature genes and proliferation-associated genes (Selfors et al., 2017) in TCGA LUSC and LUAD patient tumors (n = 1,013). Heatmap shows log2 median-centered RNA-seq gene expression data. **(B)** Correlation between proliferation score (Selfors et al., 2017) and NRF2 score in TCGA LUSC and LUAD patient tumors (n = 1,013). **(C)** Growth of a panel of lung cancer cell lines cultured in 2D. Data shown as mean ± SD from three independent experiments. Scale bar represents 400 μm. **(D)** Correlation between NRF2 score and fold change in cell number after three days culture of a panel of lung cancer cell lines from experiments described in (C). **(E)** mRNA expression of NRF2 and NQO1 relative to 2D cells in A549 or H1437 spheroids. Data shown as mean ± SD from three independent experiments, and two-tailed t-test was used to determine statistical significance ($^*p < 0.05$ and $^{**}p < 0.01$ compared to 2D).
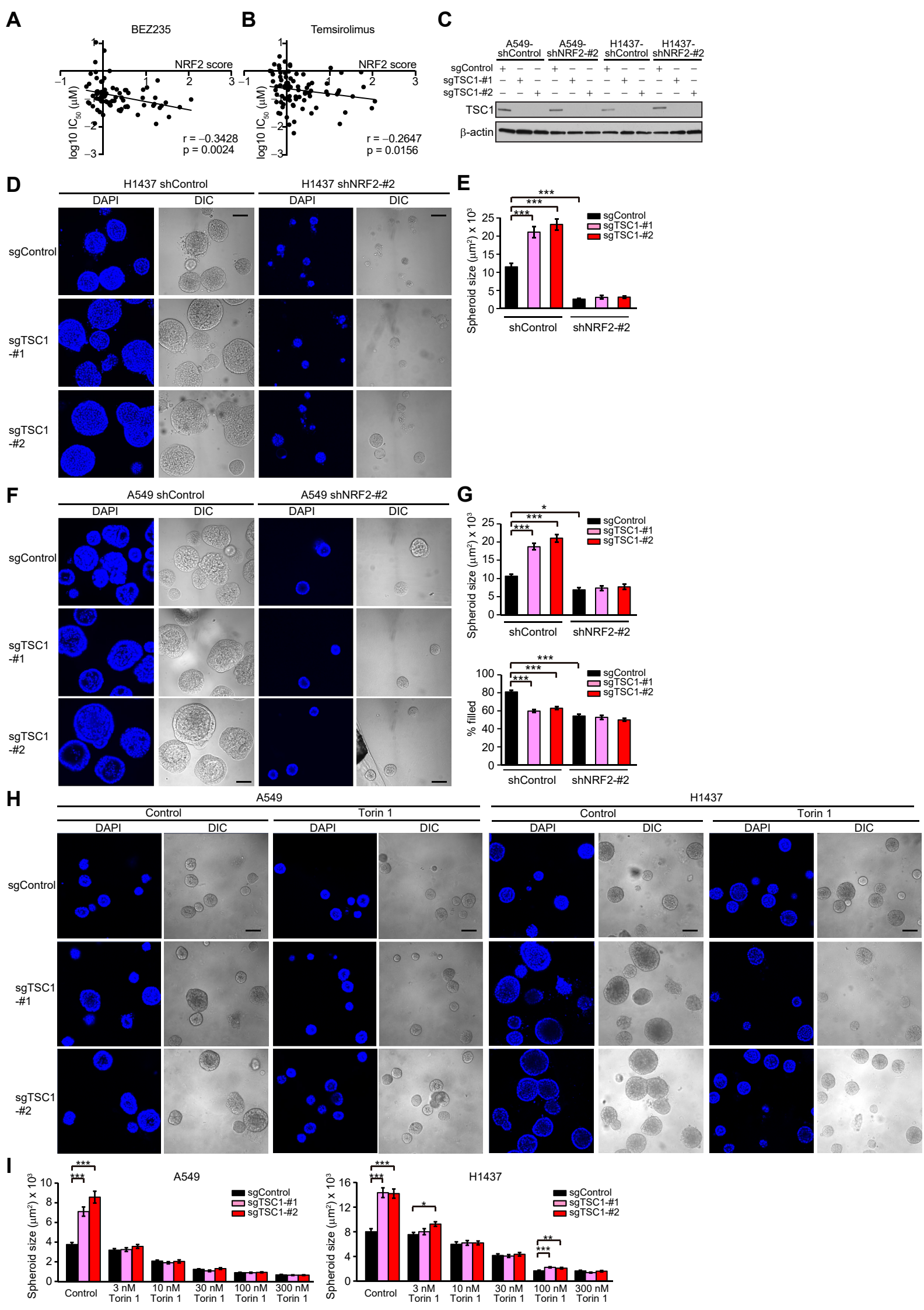
A BEZ235

NRF2 score

log10 IC$_{50}$ (μM)

r = −0.3428
p = 0.0024

B Temsirolimus

NRF2 score

log10 IC$_{50}$ (μM)

r = −0.2647
p = 0.0156

C

	A549-shControl			A549-shNRF2-#2			H1437-shControl			H1437-shNRF2-#2		
sgControl	+	−	−	+	−	−	+	−	−	+	−	−
sgTSC1-#1	−	+	−	−	+	−	−	+	−	−	+	−
sgTSC1-#2	−	−	+	−	−	+	−	−	+	−	−	+

TSC1

β-actin

D

H1437 shControl | H1437 shNRF2-#2

DAPI | DIC | DAPI | DIC

sgControl

sgTSC1-#1

sgTSC1-#2

E

Spheroid size (μm²) × 10³

*** *** ***

■ sgControl
■ sgTSC1-#1
■ sgTSC1-#2

shControl | shNRF2-#2

F

A549 shControl | A549 shNRF2-#2

DAPI | DIC | DAPI | DIC

sgControl

sgTSC1-#1

sgTSC1-#2

G

Spheroid size (μm²) × 10³

*** *** *

■ sgControl
■ sgTSC1-#1
■ sgTSC1-#2

shControl | shNRF2-#2

% filled

*** *** ***

■ sgControl
■ sgTSC1-#1
■ sgTSC1-#2

shControl | shNRF2-#2

H

A549 | | | | H1437 | | | |

Control | | Torin 1 | | Control | | Torin 1 | |

DAPI | DIC | DAPI | DIC | DAPI | DIC | DAPI | DIC

sgControl

sgTSC1-#1

sgTSC1-#2

I

Spheroid size (μm²) × 10³   A549

*** ***

■ sgControl
■ sgTSC1-#1
■ sgTSC1-#2

Control | 3 nM Torin 1 | 10 nM Torin 1 | 30 nM Torin 1 | 100 nM Torin 1 | 300 nM Torin 1

Spheroid size (μm²) × 10³   H1437

*** *** * ** ***

■ sgControl
■ sgTSC1-#1
■ sgTSC1-#2

Control | 3 nM Torin 1 | 10 nM Torin 1 | 30 nM Torin 1 | 100 nM Torin 1 | 300 nM Torin 1

Figure S3. Loss of TSC1 Promotes Proliferation but Not Survival of Inner Cells in Spheroids, Related to Figure 4.

(A and B) Correlation of NRF2 score with sensitivity to the PI3K/mTOR inhibitor BEZ235 (A) or the rapamycin analog Temsirolimus (B) in 76 (BEZ235) and 83 (Temsirolimus) lung cancer cell lines. **(C)** Immunoblot analysis of TSC1 in the indicated A549 and H1437 cells cultured in 2D. **(D)** Representative confocal images of the indicated day-12 H1437 spheroids stained with DAPI from two independent experiments. **(E)** Quantification of spheroid size from experiments described in (D) (n = 69–113). **(F)** Representative confocal images of the indicated day-12 A549 spheroids stained with DAPI from two independent experiments. **(G)** Quantification of spheroid size (n = 92–234) and percentage of filled inner space (n = 73–135) from experiments described in (F). **(H)** Representative confocal images of the indicated day-8 spheroids stained with DAPI from two independent experiments. A549 spheroids were treated with or without 3 nM Torin1 throughout the experiments. H1437 spheroids were treated with or without 10 nM Torin1 throughout the experiments. **(I)** Quantification of spheroid size in the indicated day-8 A549 (n = 40–78) and H1437 spheroids (n = 60–130). Spheroids were treated with or without Torin1 throughout the experiments. Two-tailed t-test was used to determine statistical significance. In (E) and (G), one-way ANOVA was used to determine statistical significance. In (C–I), the cells were treated with 1 μg/ml doxycycline throughout the experiments. In (D), (F), and (H), scale bar represents 100 μm. All data shown as mean ± SEM. $^{*}p < 0.05$, $^{**}p < 0.01$, and $^{***}p < 0.001$.
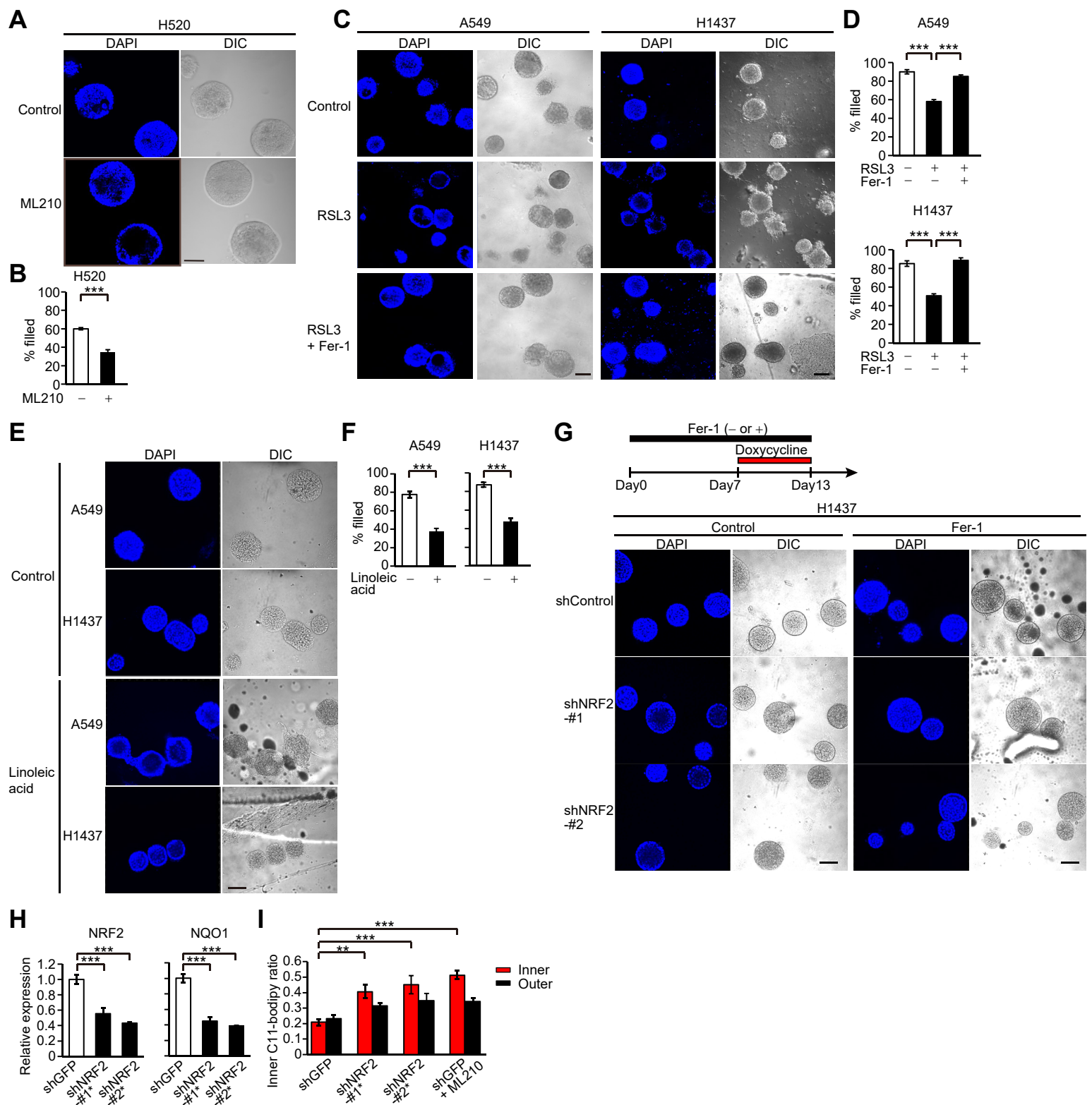
Figure S4. Inner Cells of Lung Cancer Spheroids Are Vulnerable to Ferroptosis, Related to Figure 5.
(A) Representative confocal images of day-16 H520 spheroids stained with DAPI from two independent experiments. Spheroids were treated with or without 10 μM ML210 for the last three days. **(B)** Percentage of filled inner space from experiments described in (A) (n = 12–13). **(C)** Representative confocal images of the indicated day-12 spheroids stained with DAPI from two independent experiments. Spheroids were treated with or without either 1 μM RSL3 or 1 μM RSL3 and 1 μM Fer-1 for the last three days. **(D)** Percentage of filled inner space from experiments described in (C) (n = 22–36). **(E)** Representative confocal images of day-12 A549 and day-8 H1437 spheroids stained with DAPI from two independent experiments. Spheroids were treated with or without 50 μM linoleic acid for the entire duration of the 3D culture. **(F)** Percentage of filled inner space from experiments described in (E) (n = 6–13). **(G)** Representative confocal images of the indicated day-13 H1437 spheroids stained with DAPI from three independent experiments. The spheroids were treated with 1 μg/ml doxycycline for the last six days and with either vehicle or 1 μM Fer-1 for 13 days. **(H)** mRNA expression of NRF2 and NQO1 in A549 cells transduced with shGFP, shNRF2-#1*, or shNRF2-#2*, which are not inducible shRNAs. Data were normalized to shGFP and shown as mean ± SD from four independent experiments. **(I)** Quantification of C11-Bodipy ratio from experiments described in Figure 5I (n = 12–20). In (A), (C), (E), and (G), scale bar represents 100 μm. In (B), (F), and (H), unpaired two-tailed t-test was used to determine statistical significance. In (D) and (I), one-way ANOVA was used to determine statistical significance. **p < 0.01 and ***p < 0.001. All data shown as mean ± SEM unless otherwise indicated.
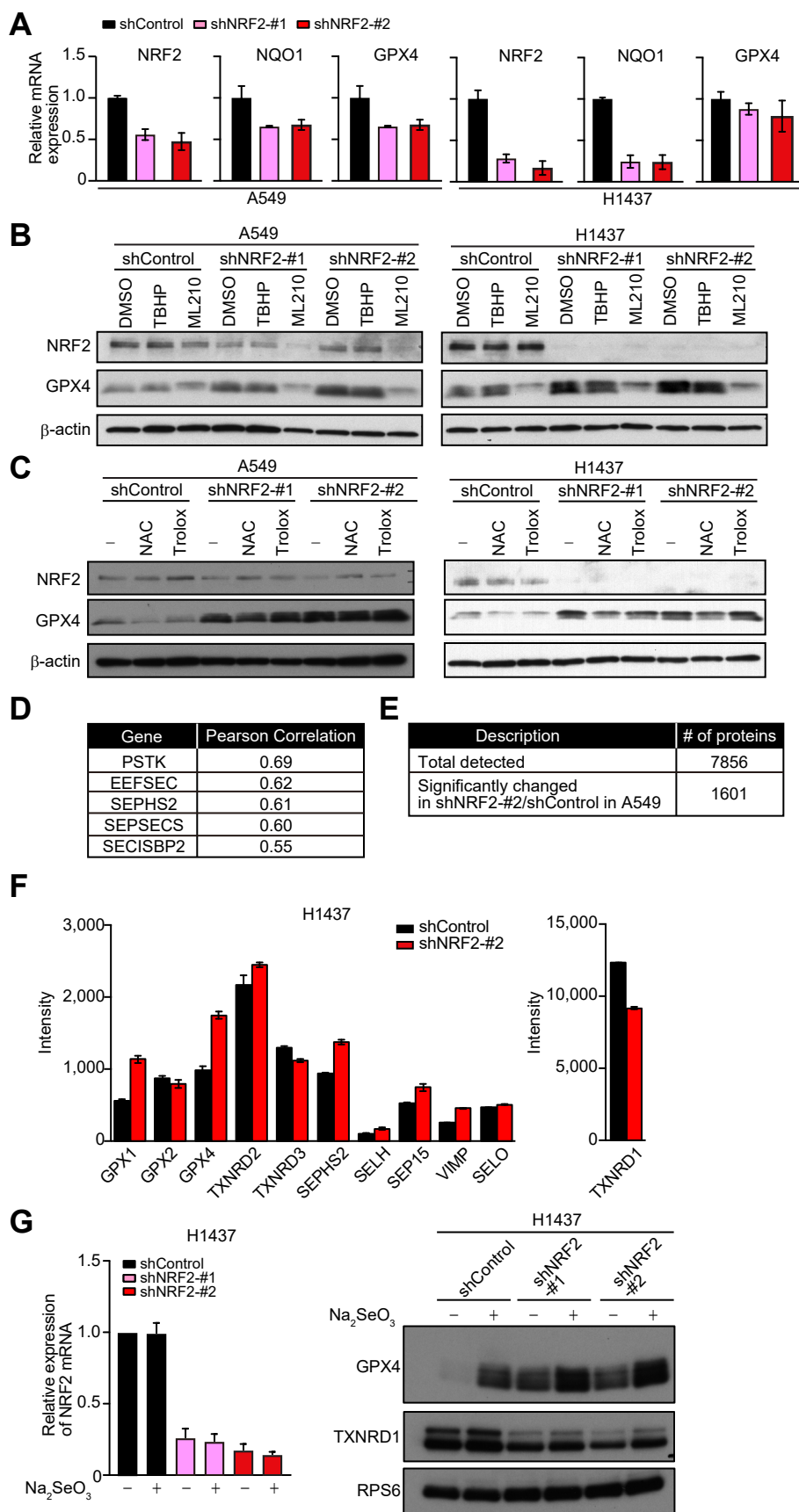
Figure S5. NRF2 Downregulation Induces Global Enrichment of Selenoproteins, Related to Figure 6.
(A) mRNA expression of NRF2, NQO1, and GPX4 in the indicated cells upon treatment with 1 μg/ml doxycycline for 72 hours in 2D culture. Data were normalized to shControl and shown as mean ± SEM from two independent experiments. **(B and C)** Immunoblot analysis of NRF2 and GPX4 in the indicated cells in the presence of 1 μg/ml doxycycline. In (B), the cells were treated with 10 μM TBHP (for 48 hours) or 10 μM ML210 (72 hours) in 2D culture. In (C), the cells were treated with 5 mM NAC or 250 μM Trolox for 72 hours in 2D culture. **(D)** Top co-dependencies of GPX4, which are genes required for Sec biosynthesis, based on CRISPR (Avana) Public Release 19Q2 via DepMap. **(E)** Summary of proteomics data. **(F)** Intensity of all selenoproteins detected in the indicated cells after 72-hour doxycycline (1 μg/ml) treatment. Data shown as mean ± SD from two (shControl) or three (shNRF2-#2) technical replicates. **(G)** mRNA expression of NRF2 and immunoblot analysis of GPX4 and TXNRD1 in the indicated H1437 treated with either 1 μg/ml doxycycline or both 1 μg/ml doxycycline and 30 nM Na_2SeO_3 for 72 hours in 2D culture. For qPCR analysis, data were normalized to shControl cells without Na_2SeO_3 treatment and shown as mean ± SEM. Both qPCR and immunoblot analyses are from three independent experiments.
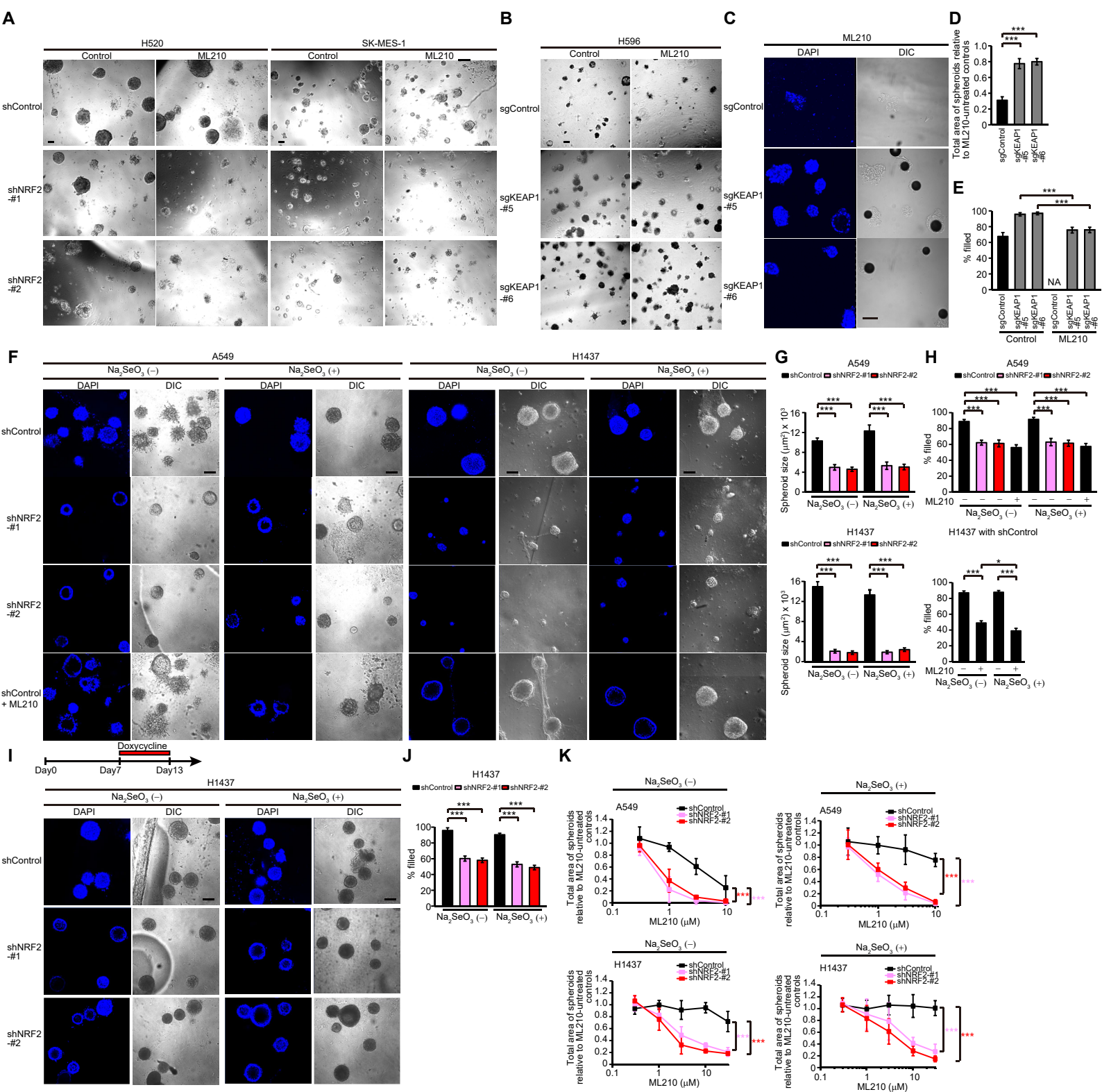
A

H520 | SK-MES-1

Control | ML210 | Control | ML210

shControl
shNRF2-#1
shNRF2-#2

B

H596

Control | ML210

sgControl
sgKEAP1-#5
sgKEAP1-#6

C

ML210

DAPI | DIC

sgControl
sgKEAP1-#5
sgKEAP1-#6

D

Total area of spheroids relative to ML210-untreated controls

sgControl / sgKEAP1-#5 / sgKEAP1-#6

*** ***

E

% filled

*** ***

sgControl / sgKEAP1-#5 / sgKEAP1-#6 — Control
sgControl / sgKEAP1-#5 / sgKEAP1-#6 — ML210 (NA)

F

A549 | H1437

Na_2SeO_3 (−) | Na_2SeO_3 (+) | Na_2SeO_3 (−) | Na_2SeO_3 (+)

DAPI | DIC | DAPI | DIC | DAPI | DIC | DAPI | DIC

shControl
shNRF2-#1
shNRF2-#2
shControl + ML210

G

A549

shControl / shNRF2-#1 / shNRF2-#2

Spheroid size (μm^2) x 10^3

*** *** ***

Na_2SeO_3 (−) | Na_2SeO_3 (+)

H1437

Spheroid size (μm^2) x 10^3

*** *** ***

Na_2SeO_3 (−) | Na_2SeO_3 (+)

H

A549

shControl / shNRF2-#1 / shNRF2-#2

% filled

*** *** *** ***

ML210 − − + | − − +
Na_2SeO_3 (−) | Na_2SeO_3 (+)

H1437 with shControl

% filled

*** *** *

ML210 − + | − +
Na_2SeO_3 (−) | Na_2SeO_3 (+)

I

Day0 | Day7 | Day13
Doxycycline

H1437

Na_2SeO_3 (−) | Na_2SeO_3 (+)

DAPI | DIC | DAPI | DIC

shControl
shNRF2-#1
shNRF2-#2

J

H1437

shControl / shNRF2-#1 / shNRF2-#2

% filled

*** *** ***

Na_2SeO_3 (−) | Na_2SeO_3 (+)

K

Na_2SeO_3 (−)

A549

Total area of spheroids relative to ML210-untreated controls

shControl / shNRF2-#1 / shNRF2-#2

ML210 (μM)

*** ***

Na_2SeO_3 (+)

A549

Total area of spheroids relative to ML210-untreated controls

shControl / shNRF2-#1 / shNRF2-#2

ML210 (μM)

*** ***

Na_2SeO_3 (−)

H1437

Total area of spheroids relative to ML210-untreated controls

shControl / shNRF2-#1 / shNRF2-#2

ML210 (μM)

*** ***

Na_2SeO_3 (+)

H1437

Total area of spheroids relative to ML210-untreated controls

shControl / shNRF2-#1 / shNRF2-#2

ML210 (μM)

*** ***

Figure S6. High NRF2 Activity Induces Resistance to ML210 in Spheroids, Related to Figure 7.

(A) Representative images of the indicated day-16 spheroids from two independent experiments. The spheroids were treated with or without 10 μM ML210 for the last three days. **(B)** Representative images of the indicated day-14 spheroids from two independent experiments. The spheroids were treated with or without 3 μM ML210 for the last three days. **(C)** Representative confocal images of the indicated day-12 H596 spheroids stained with DAPI from two independent experiments. The spheroids were treated with or without 3 μM ML210 for the last three days. **(D and E)** Total area of the spheroids relative to ML210-untreated controls (D) and percentage of filled inner space (E) from experiments described in (C) [n = 18–62 for (D) and n = 24–73 for (E)]. The data for ML210-untreated spheroids is from Figures 2I and 2J as these experiments were performed concurrently as the experiment presented in Figures S6C–S6E. In (E), it was not technically feasible to assess % filled in ML210-treated H596 spheroids with sgControl because of the induction of cell death and the loss of spheroid structure by ML210 treatment. **(F)** Representative confocal images of the indicated day-12 spheroids from two independent experiments. The spheroids were treated with or without 30 nM Na_2SeO_3 for 12 days and with either vehicle, 3 μM ML210 (A549), or 10 μM ML210 (H1437) for the last three days. **(G)** Quantification of spheroid size from experiments described in (F) (n = 25–45). **(H)** Percentage of filled inner space from experiments described in (F) (n = 28–50). **(I)** Representative confocal images of the indicated spheroids from two independent experiments. The spheroids were treated with or without 30 nM Na_2SeO_3 for 13 days. The timeline of doxycycline treatment (1 μg/ml) is shown. **(J)** Percentage of filled inner space from experiments described in (I) (n = 27–49). **(K)** Total area of spheroids relative to ML210-untreated controls in the indicated spheroids treated with ML210 for the last three days. A549 and H1437 cells were cultured in the presence or absence of 30 nM Na_2SeO_3 for 12 days. Data shown as mean ± SD from three independent experiments, and two-way ANOVA was used to determine statistical significance. In (A), (F)–(H), and (K), the spheroids were treated with 1 μg/ml doxycycline throughout the experiments. In (A)–(C), (F), and (I), scale bar represents 100 μm. In (D), (E), (G), (H), and (J), data shown as mean ± SEM. In (D) and (E), unpaired two-tailed t-test was used to determine statistical significance. In (G), (H), and (J), one-way ANOVA was used to determine statistical significance. ***$p < 0.001$.
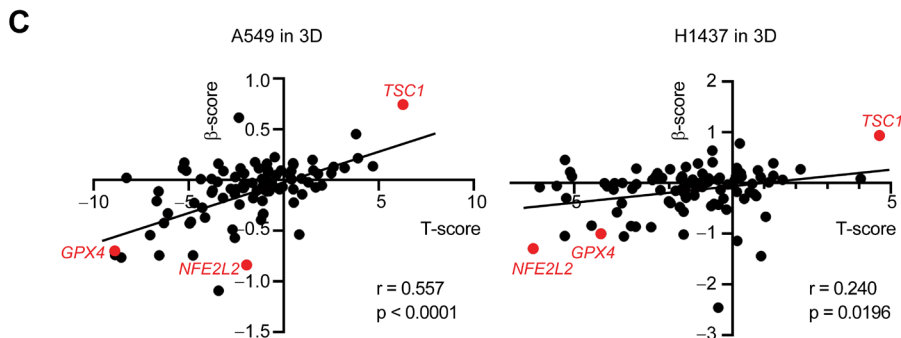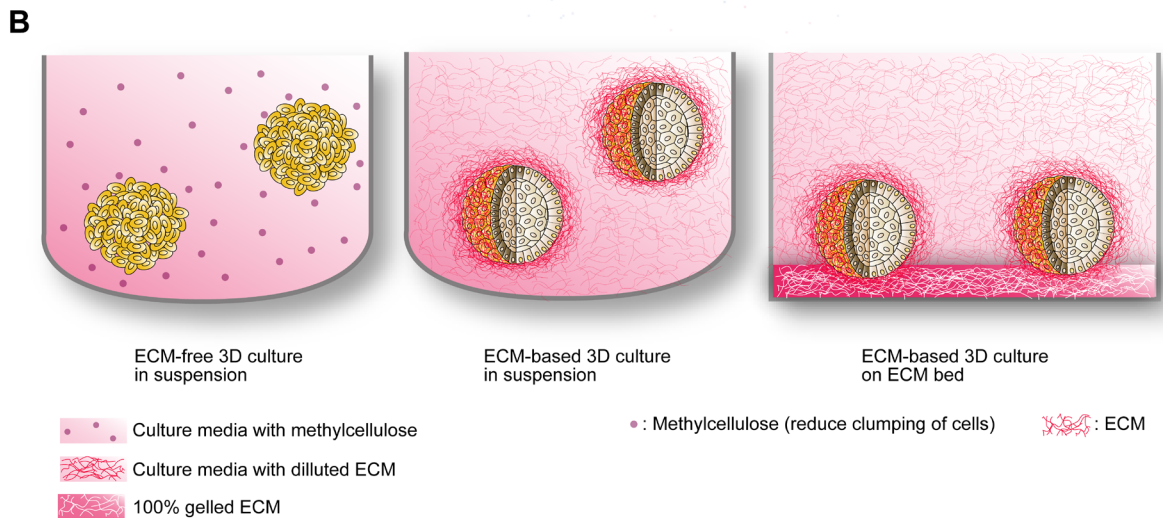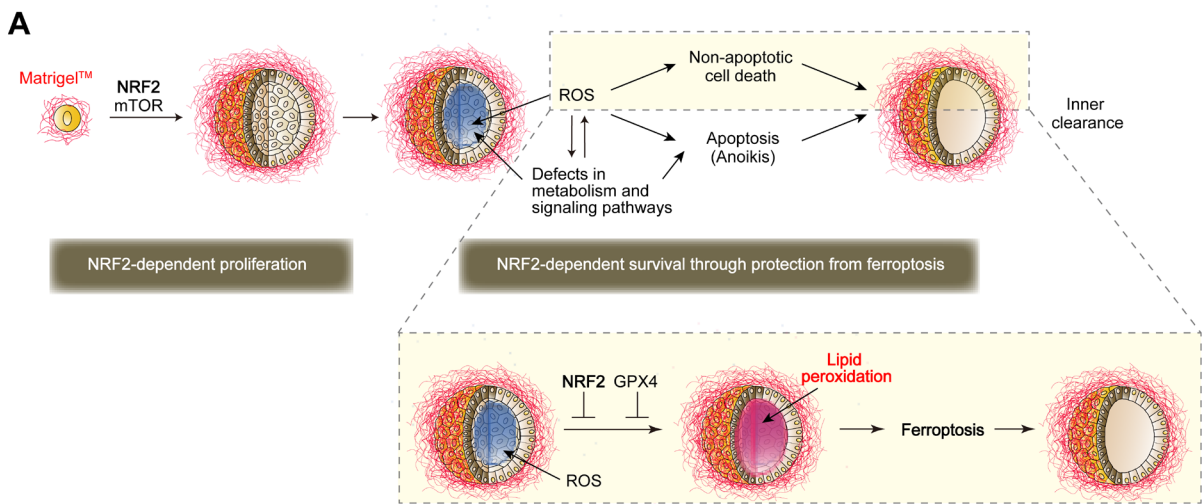
Figure S7. Model of the NRF2-Induced Spheroid Formation in Lung Cancer, Related to Figures 1–7.
(A) High NRF2 activity is necessary for both spheroid formation overall and the specific survival of centrally-localized spheroid cells in lung cancer. NRF2 and mTOR cooperatively induce proliferation of spheroid cells through mechanisms distinct from, or only indirectly related to, antioxidant programs. Both NRF2 and GPX4 prevent ferroptosis, a non-apoptotic form of cell death, outside the natural matrix niches through redox regulation, leading to the filled spheroid structure. **(B)** Diagram illustrating differences in 3D culture methods utilized in our study and that of Han et al (Han et al., 2020). In the CRISPR screens reported in the Han et al. publication, cells formed 3D structures in medium without exogenous ECM, conditions that require anchorage-independent proliferation and survival (left panel). In our CRISPR screens, we utilized a reconstituted basement membrane ECM (Matrigel™)-based 3D culture, which is typically used for organoid and other 3D models, in order to better model in vivo cell-to-ECM interaction as well as cell-to-cell interaction (middle panel). For our confocal imaging and drug assessment, we utilized Matrigel™ bed as well as culture media with diluted Matrigel™ in order to efficiently assess phenotypes of spheroids in a single spheroid level (right panel). **(C)** Correlation between the β-scores from our CRISPR screens and T-scores from the CRISPR screens from the Han et al. report (Han et al., 2020). The 93 genes that overlap between our 1,500 CRISPR gene list and their top 911 gene list are shown.